ESR spectroscopy of Co^{2+} impurities in $Cd_2P_2S_6$ and $Cd_2P_2Se_6$

ESR spectroscopy of Co²⁺ impurities in Cd₂P₂S₆ and Cd₂P₂Se₆

G T Long and D A Cleary

Chemistry Department, Washington State University, Pullman, Washington 99164–4630, USA

Abstract. The ESR spectra of Co²⁺ impurities in Cd₂P₂S₆ and Cd₂P₂Se₆ are reported. The Co²⁺ ion is an $S = \frac{3}{2}$ ion and substitutes for Cd²⁺ ($S = 0$) ions in the Cd₂P₂X₆ crystal. The spin Hamiltonian parameters g and A were determined using an effective spin $= \frac{1}{2}$. For Cd₂P₂S₆, $g_\parallel = 4.86$, $A_\parallel = 440$ MHz, $g_\perp = 4.01$ and $A_\perp = 346$ MHz. For Cd₂P₂Se₆, $g_\parallel = 4.98$, $A_\parallel = 565$ MHz, $g_\perp = 3.85$ and $A_\perp = 250$ MHz. From the temperature dependence of the linewidth, the zero-field splitting, $2D$, for Co²⁺ doped into Cd₂P₂S₆ is estimated to be 127 cm⁻¹. The individual hyperfine lines of Co²⁺ doped into Cd₂P₂Se₆ show superhyperfine structure due to ⁷⁷Se ($I = \frac{1}{2}$, 7.58% natural abundance). This additional splitting is consistent with some covalent bonding between the Co²⁺ and its six selenium ligands.

1. Introduction

The transition metal phosphorus chalcogenides, $M_2P_2X_6$, where M is a transition metal and X is sulphur or selenium, are currently enjoying considerable attention. The interest in these materials stems from their ability to undergo intercalation reactions. Intimately connected with these intercalation studies are efforts to characterise the pure, unintercalated $M_2P_2X_6$ lattices. Characterisation of pure $M_2P_2X_6$ lattices has included single-crystal x-ray diffraction [1], magnetic susceptibility [2], ³¹P NMR [3], x-ray photoelectron spectroscopy [4], optical absorption and emission [5], IR and Raman spectroscopy [6], Mössbauer spectroscopy [7], neutron diffraction [8], and ESR [9]. One of the objectives of these studies is to characterise the highest occupied and lowest unoccupied electronic states in the $M_2P_2X_6$ lattices. This is of crucial importance because of the role such states play in the redox intercalation reactions of these lattices.

ESR investigations of $M_2P_2X_6$ lattices divide into two types. In the first, the pure $M_2P_2X_6$ material is studied. The ESR spectrum of a compound such as $Mn_2P_2S_6$ consists of a single, broad, intense line [10, 11]. Because of the high concentration of spins in this sample, spin–spin interactions obliterate all of the fine structure and hyperfine structure usually associated with the ESR spectrum of Mn²⁺. Useful information, however, can still be obtained. For example, the peak-to-peak linewidth in the case of $Mn_2P_2S_6$ diverges as the sample orders antiferromagnetically below 78 K.

The other type of $M_2P_2X_6$ ESR investigation, and the one employed in this study, utilises an ESR spin-labelled lattice. In such an experiment, a diamagnetic host is prepared with a trace amount of paramagnetic probe ions. The assumption is that the magnetic

parameters determined for the paramagnetic impurity ions are close to those for the corresponding pure paramagnetic compound. This technique of spin dilution has been used for many years in solid state ESR [12], and has recently been adopted in the study of the transition metal phosphorus chalcogenides [13, 14]. In this recent work, the ESR spectrum of Mn^{2+} doped into $Cd_2P_2S_6$ and $Cd_2P_2Se_6$ was investigated.

The work presented in this paper involves the dilution of Co^{2+} spins into $Cd_2P_2S_6$ and $Cd_2P_2Se_6$. Presumably, the magnetic parameters determined for the Co^{2+} ions, such as g, A, and D, are also the parameters for $Co_2P_2S_6$ and $Co_2P_2Se_6$. In addition, because the Co^{2+} hyperfine lines are further split by ^{77}Se, we conclude that the unpaired d electrons formally assigned to the Co^{2+} are delocalised among the six coordinating selenium ligands in $Co_2P_2Se_6$. The degree of delocalisation has yet to be determined.

The work presented here is important because it demonstrates the potential for characterising the Fermi level of the transition metal phosphorus chalcogenides using ESR spectroscopy. In particular, the orbital overlap between the metal ions and the chalcogenide ligands can be evaluated. This metal–chalcogenide interaction is important for understanding the redox intercalation reactions that $M_2P_2X_6$ lattices undergo.

2. Experimental details

The spin-labelled $Cd_2P_2S_6$ and $Cd_2P_2Se_6$ were grown by chemical vapour transport using iodine as the transporting agent. The elements (Cd, Co, P (red), and S or Se) were weighed out such that the stoichiometry of the mixture before reaction was

$$Cd_{95}Co_5P_{100}X_{300}.$$
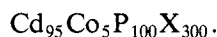
The final crystals contained much less cobalt than this (see below). Iodine was added such that the concentration was 5 mg cm^{-3}. The crystals were grown in a temperature gradient of 650–600 °C/15 cm for $\approx$5 days. The $Cd_2P_2S_6$ crystals were transparent and colourless, and the $Cd_2P_2Se_6$ crystals were transparent and orange. Typical sample size for ESR studies was $2 \times 2 \times 0.05$ mm^3.

ESR spectra were recorded on a Varian E-9 spectrometer operating at X-band interfaced to an IBM PC/XT. An Air Products Heli-Tran system was used for variable-temperature work down to 6 K. The microwave frequency was measured with a Systron–Donner model 6520 counter. The magnetic field was measured with a Micro-Now NMR gaussmeter. The magnetic field was modulated at 10 kHz. The microwave power was adjusted to avoid saturation effects. At the lowest temperature, 6 K, the power was reduced to 0.01 mW.

The chemical analysis was accomplished via electron microbeam analysis. The analysis was done on an Camex electron microprobe using a 20 μm beam diameter at 15 kV. The elements cadmium, phosphorus, sulphur, and cobalt were analysed simultaneously. The weight per cent is determined to a precision of $\pm 0.05\%$. The electron beam penetrates to a depth of a few μm and therefore samples several thousand unit cells. Microprobe analysis is not regarded as a surface technique.

The ESR parameters were determined using a program by Gladney and Swalen from the Quantum Chemical Program Exchange [15].

Table 1. Spin Hamiltonian parameters for Co^{2+} doped $Cd_2P_2X_6$ lattices.

Host	$g_\parallel$	$g_\perp$	$A_\parallel$ (MHz)	$A_\perp$ (MHz)	$2D$ (cm^{-1})
$Cd_2P_2S_6$	4.86	4.01	440	346	127
$Cd_2P_2Se_6$	4.98	3.85	565	250	169†

† Estimated as described in the text.

Magnetic Field (Gauss)
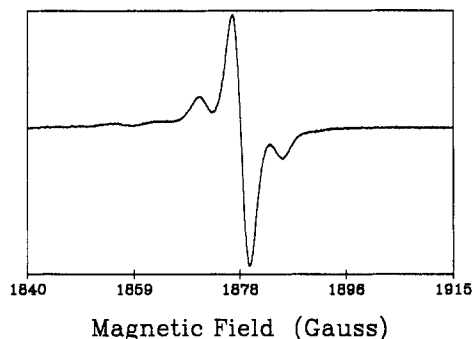
Figure 1. ESR spectrum of the high-field line in the perpendicular orientation of Co^{2+}-doped $Cd_2P_2Se_6$. Twenty five scans have been signal averaged in this spectrum. The splitting due to ^{77}Se is ≈ 10 G. Temperature = 6 K.

3. Results

$Cd_2P_2S_6$ and $Cd_2P_2Se_6$ are layered materials with close-packed layers of chalcogenides. Crystals of these materials can be grown up to 1 cm × 1 cm × 0.01 cm. The small dimension of these crystals is along the stacking axis making it easy to determine the orientation of the stacking axis with respect to an external reference frame.

The ESR spectra of Co^{2+} doped into $Cd_2P_2S_6$ and $Cd_2P_2Se_6$ single crystals are consistent with the Co^{2+} ions substituting for Cd^{2+} ions. A normal eight-line spectrum was observed for all orientations of the crystal. The linewidths at 6 K were approximately 4 G in all cases except for $Cd_2P_2S_6$ at $\theta = 0°$ where the linewidths were 8 G. It is known from the single-crystal data for $Cd_2P_2S_6$ that the cadmium occupies a site of trigonally distorted octahedral symmetry (D_{3d}) [16]. As is often the case with high-spin Co^{2+}, the zero-field splitting is very large compared with a nominal Zeeman splitting of 0.3 cm^{-1} [14]. Therefore instead of using $S = \frac{3}{2}$ when diagonalising the spin Hamiltonian matrix (2), an effective $S' = \frac{1}{2}$ can be used. The g and A-values listed in table 1 where determined in this manner.

From the angle dependence of the ESR spectrum, one can conclude that the Co^{2+} resides in a site of axial symmetry, which is consistent with replacing Cd^{2+}. The ESR spectra of Co^{2+} doped into $Cd_2P_2Se_6$ are qualitatively similar to the spectra from doping into $Cd_2P_2S_6$ with one important exception; the individual hyperfine lines are further split in $Cd_2P_2Se_6$ by the $I = \frac{1}{2}$ (7.58% natural abundance) ^{77}Se isotope [17]. One of these lines is shown in figure 1 ($\theta = 90°$). The additional splitting is ≈ 10 G.
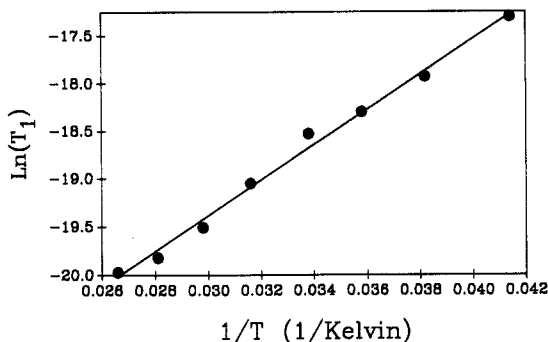
Figure 2. A plot of $\ln(T_1)$ versus inverse absolute temperature, $1/T$, for the perpendicular orientation of Co^{2+} doped into $Cd_2P_2S_6$. The slope of this line yields $2D$ in K.

The ESR spectra were analysed using the following spin Hamiltonian [14]:

$$\hat{H} = \beta H \, \mathbf{g} \, \hat{S} + h \hat{S} \, \mathbf{A} \, \hat{I} \tag{1}$$

where the symbols have their usual meaning. For the case of axial symmetry, this Hamiltonian can be simplified to

$$\hat{H} = \beta g_\parallel H_z \hat{S}_z + \beta g_\perp H_x \hat{S}_x + h[A_\parallel \hat{S}_z \hat{I}_z + A_\perp (\hat{S}_x \hat{I}_x + \hat{S}_y \hat{I}_y)]. \tag{2}$$

The parameters $g_\parallel$, $g_\perp$, $A_\parallel$, and $A_\perp$ were determined using the Gladney and Swalen program obtained from the Quantum Chemical Program Exchange [13]. These values are listed in table 1. The calculated and observed line positions agree within 1 G other than for $Cd_2P_2Se_6$ at $\theta = 90°$ where differences up to 12 G were obtained. The value of $2D$ for the $Cd_2P_2S_6$ case was determined using the method of Zverev and Prokhorov [18]. This method consists of expressing the individual hyperfine linewidth as a function of a constant term and a temperature-dependent term:

$$\Delta H_{P-P} = \Delta H_{constant} + \Delta H(T) \tag{3}$$

where $\Delta H(T)$ is due to spin–lattice relaxation, T_1. Values of T_1 were obtained from the relation

$$T_1(T) = C/\Delta H(T). \tag{4}$$

The magnitude of $2D$ is determined from the relation

$$T_1 \text{ (s)} = 5.9 \times 10^{-12} \exp(2D/kT). \tag{5}$$

The slope of the plot of $\ln(T_1)$ versus $1/T$ (K^{-1}) (see figure 2) yields $2D = 127 \pm 8 \text{ cm}^{-1}$ (note that the value of C does not need to be determined). This analysis holds for either the parallel or the perpendicular orientation and results in the same value of $2D$.

From the chemical analysis of the $Cd_2P_2S_6$ doped sample, the stoichiometry can be written as

$$Cd_{98.4}P_{99.7}S_{300}Co_{0.3}$$
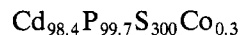
with an uncertainty in each number of $\pm2\%$. The $Cd_2P_2Se_6$ doped sample was not chemically analysed, but from the signal-to-noise ratio of the Co^{2+} ESR spectrum, we estimate that the cobalt concentration is approximately one half of what it is in the

Cd$_2$P$_2$S$_6$ sample. In both cases, the cobalt–cobalt interactions are considered negligible. This is important because Co$_2$P$_2$S$_6$ orders antiferromagnetically at 122 K [19].

4. Discussion

The value of the zero-field splitting, D, can be determined from the temperature dependence of the individual hyperfine linewidths. With this value of D, the spin Hamiltonian appropriate for $S = \frac{3}{2}$ can be used:

$$\hat{H} = \beta H \mathbf{g} \hat{S} + \hat{S} \mathbf{D} \hat{S} + h\hat{S} \mathbf{A} \hat{I}. \tag{6}$$

This analysis affects the values in table 1 such that the $g_\perp$ and the $A_\perp$ are reduced by $\frac{1}{2}$. The parallel parameters are unaffected since there is no mixing of the $\pm\frac{3}{2}\rangle$ states with the $\pm\frac{1}{2}\rangle$ states in the parallel orientation.

As mentioned above, the method used to determine the zero-field splitting in the Cd$_2$P$_2$S$_6$ case does not work in the Cd$_2$P$_2$Se$_6$ case because of the additional splitting of the hyperfine lines by ^{77}Se nuclei. However, the zero-field splitting can be estimated if it is assumed to be proportional to $(g_\parallel - g_\perp)$ [20]:

$$D = C(g_\parallel - g_\perp). \tag{7}$$

The value of the proportionality constant is determined from the Cd$_2$P$_2$S$_6$ case where D, $g_\parallel$, and $g_\perp$ are known. The estimated value of $2D$ listed for the Cd$_2$P$_2$Se$_6$ case was determined using this procedure. As expected from previous work, the zero-field splitting increases as the covalency of the metal–ligand bond increases [9]. However, an important feature of the Cd$_2$P$_2$Se$_6$–Co^{2+} ESR spectra is inconsistent with this conclusion; the parallel hyperfine splitting, $A_\parallel$, is *greater* in Cd$_2$P$_2$Se$_6$ than in Cd$_2$P$_2$S$_6$. This indicates that the spin density on Co^{2+} is greater in the selenide lattice than in the sulphide lattice, which translates into a *less* covalent cobalt–chalcogenide bond in Cd$_2$P$_2$Se$_6$ than in Cd$_2$P$_2$S$_6$. This is unlikely given that the electronegativity of cobalt is closer to selenium than to sulphur [21]. The resolution to this problem may be in the determination of the spin Hamiltonian parameters for the selenide case.

5. Conclusion

The ESR spectra of Co^{2+} ions doped into Cd$_2$P$_2$S$_6$ and Cd$_2$P$_2$Se$_6$ have been recorded. The spectra are consistent with Co^{2+} ions substituting for Cd^{2+} ions in the host lattice. From the temperature dependence of the linewidth, the zero-field splitting of Co^{2+} ions doped into Cd$_2$P$_2$S$_6$ has been determined. The zero-field splitting for Co^{2+} doped into Cd$_2$P$_2$Se$_6$ has been estimated from the difference $g_\parallel - g_\perp$. Additional splitting of the Co^{2+} hyperfine lines by ^{77}Se indicates some covalent bonding between cobalt and selenium.

References

[1] Ouvrard G, Brec R and Rouxel J 1985 *Mater. Res. Bull.* **20** 1181
[2] Clément R, Girerd J J and Morgenstern-Badarau I 1980 *Inorg. Chem.* **19** 2852
[3] Berthier C, Chabre Y and Minier M 1978 *Solid State Commun.* **28** 327
[4] Piacentini M, Grasso V, Santangelo S, Fanfoni M, Modesti S and Savoia A 1984 *Nuovo Cimento* **4** 444

[5] Boerio-Goates J, Lifshitz E and Francis A H 1981 *Inorg. Chem.* **20** 3019
[6] Sourisseau C, Forgerit J P and Mathey Y 1983 *J. Solid State Chem.* **49** 134
[7] Jernberg P, Bjarman S and Wappling R 1984 *J. Magn. Magn. Mater.* **46** 178
[8] Wiedenmann A, Rossat-Mignod J, Louisy A, Brec R and Rouxel J 1981 *Solid State Commun.* **40** 1067
[9] Cleary D A, Francis A H and Lifshitz E 1986 *Chem. Phys.* **106** 123
[10] Okuda K, Kurosawa K, Saito S, Honda M, Yu Z and Date M 1986 *J. Phys. Soc. Japan* **55** 4456
[11] Kim K and Cleary D A 1990 *J. Phys. Chem.* at press
[12] Abragam A and Bleaney B 1970 *Electron Paramagnetic Resonance of Transition Metal Ions* (New York: Oxford University Press)
[13] Lifshitz E and Francis A H 1982 *J. Phys. Chem.* **86** 4714
[14] Lifshitz E, Cleary D A and Francis A H 1988 *Chem. Phys.* **127** 305
[15] Gladney H M and Swalen J D 1969 *Quant. Chem. Program Exch.* **11** 134
[16] Ouvrard G, Brec R and Rouxel J 1985 *Mater. Res. Bull.* **20** 1181
[17] Wertz J E and Bolton J R 1972 *Electron Spin Resonance: Elementary Theory and Practical Applications* (New York: McGraw-Hill)
[18] Zverev G M and Prokhorov A M 1963 *Paramagnetic Resonance* vol 1, ed H Low (New York: Academic) p 13
[19] Brec R 1986 *Solid State Ion.* **22** 3
[20] von Bardeleben H J, Schwab C and Feigelson R S 1982 *J. Phys. C: Solid State Phys.* **15** 5269
[21] *Lange's Handbook of Chemistry* 1985 13th edn, ed J A Dean (New York: McGraw-Hill) pp 3–11